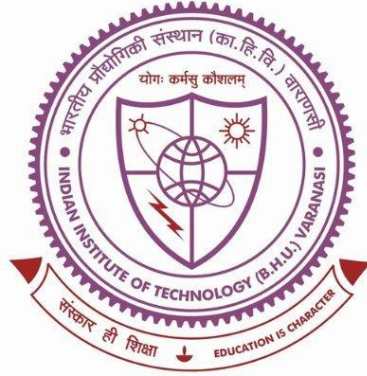


Tribological studies of multilayer and nanocomposite coatings



*Thesis submitted in partial fulfillment
for the Award of Degree*

Doctor of Philosophy

In

Mechanical Engineering

By

AMOD KASHYAP

**DEPARTMENT OF MECHANICAL ENGINEERING
INDIAN INSTITUTE OF TECHNOLOGY
(BANARAS HINDU UNIVERSITY)
VARANASI – 221005**

16131501

2022



**INDIAN INSTITUTE OF TECHNOLOGY (BANARAS
HINDU UNIVERSITY) VARANASI
VARANASI-221005**

CERTIFICATE

It is certified that the work contained in the thesis titled “**Tribological studies of multilayer and nanocomposite coatings**” by **Mr. Amod Kashyap** (Roll No. 16131501) has been carried out under my supervision and this work has not been submitted elsewhere for a degree.

It is further certified that the student has fulfilled all the requirements of Comprehensive Examination, Candidacy and SOTA for the award of Ph.D. Degree.

Prof. A. P. Harsha
(Supervisor)

Department of Mechanical Engineering
Indian Institute of Technology
(Banaras Hindu University) Varanasi
Varanasi-221005, India

Dr. Harish C. Barshilia
(Co-Supervisor)

CSIR-National Aerospace Laboratories,
Bengaluru- 560017,
Karnataka, India



INDIAN INSTITUTE OF TECHNOLOGY
(BANARAS HINDU UNIVERSITY) VARANASI
VARANASI-221005

DECLARATION BY THE CANDIDATE

I, Amod Kashyap, certify that the work embodied in this thesis is my own bona fide work and carried out by me under the supervision of Prof. A. P. Harsha and Dr. Harish C. Barshilia from December 2016 to September 2022, at the Department of Mechanical Engineering, Indian Institute of Technology (BHU), Varanasi. The matter embodied in this thesis has not been submitted for the award of any other degree/diploma. I declare that I have faithfully acknowledged and given credits to the research workers wherever their works have been cited in my work in this thesis. I further declare that I have not willfully copied any other's work, paragraphs, text, data, results, etc., reported in journals, books, magazines, reports dissertations, theses, etc., or available at websites and have not included them in this thesis and have not cited as my own work.

Date: 17/10/2022

Place: IIT (BHU), Varanasi

Amod
(Amod Kashyap)

CERTIFICATE FROM THE SUPERVISOR

This is to certify that the above statement made by the candidate is correct to the best of my knowledge.

Prof. A. P. Harsha
(Supervisor)

Dr. Harish C. Barshilia
(Co-Supervisor)

Dr. A.P. Harsha
Professor
Department of Mechanical Engineering
Indian Institute of Technology
(Banaras Hindu University)
Varanasi-221005, India

Prof. Santosh Kumar
Head of Department
Department of Mechanical Engineering
IIT (BHU), Varanasi-221005

Santosh Kumar
विभागाध्यक्ष/HEAD
यांत्रिक अभियंता विभाग/Deptt. of Mechanical Engg.
भारतीय प्रौद्योगिकी संस्थान/Indian Institute of Technology
(वाराणसी/B.H.U.)
वाराणसी-२२१००५/Varanasi-221005

COPYRIGHT TRANSFER CERTIFICATE

Title of the Thesis: **Tribological studies of multilayer and nanocomposite coatings**

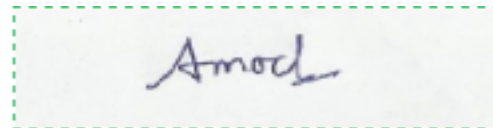
Name of the Student: **Amod Kashyap**

Copyright Transfer

The undersigned hereby assigns to the Indian Institute of Technology (Banaras Hindu University) Varanasi all rights under copyright that may exist in and for the above thesis submitted for the award of the **Doctor of Philosophy**.

Date: 17/10/2022

Place: IIT (BHU), Varanasi

A rectangular box with a dashed green border containing a handwritten signature in blue ink that reads "Amod".

(Amod Kashyap)

Note: However, the author may reproduce or authorize others to reproduce material extracted verbatim from the thesis or derivative of the thesis for author's personal use provided that the source and the Institute's copyright notice are indicated.

Acknowledgements

At the outset, let me pay my obeisance to ‘Lord Shiva’ and ‘Maa Saraswati’ for catapulting me to this level of academic pursuit. After that, I feel proud and privileged to get the chance to thank the people who played an indispensable role during this research programme. Though the success in this endeavor is the result of a number of known and unknown spirits, it is my pious duty and happiness to recall and gratefully acknowledge the great efforts and love of those few people who made this possible with their supreme strength and the power of will.

First and foremost, I would like to express my deep sense of gratitude and appreciation to my supervisors, Prof. A. P. Harsha and Dr. Harish C. Barshilia, for their esteemed guidance, invaluable encouragement, moral support, providing enough space to work on my ideas and scholarly inputs from the early stage of research work that build confidence in me during the research work. This research work would not have been possible without their valuable guidance, moral support, and continuous encouragement. I humbly acknowledge my heartfelt gratitude to them.

I am also expressing my sincere thanks to Ph.D. coursework faculty members, Prof. V. P. Singh, Dr. Cherian Samuel, and Prof. S.K. Sharma, for their kind, moral, and continuous encouragement.

I would like to express my thanks to my Research Progress Evaluation Committee (RPEC) members; Prof. R. K. Gautam, subject expert in the Department of Mechanical Engineering, and Dr. Chandana Rath, an external expert from the School of Materials Science and Technology of the Institute, for their kind cooperation, useful suggestion and insightful via comments throughout the period of research work which has been instrumental in the success of the dissertation.

I wish to acknowledge my sincere gratefulness to Prof. Santosh Kumar, Head, Department of Mechanical Engineering, Indian Institute of Technology (BHU), Varanasi, the former heads, Prof. A. P. Harsha, Prof. A. K. Jha, Prof. A. K. Agrawal for their kind gesture and extending all sorts of facilities in the Department to pursue this kind of research work. I am also thankful to Convener DPGC, Dr. Arnab Sarkar, the former Convener DPGC, Dr. U.S. Rao, Prof. R. K. Gautam, Prof. Rajesh Kumar, Prof. A. P. Harsha, and all respected DPGC members for their kind support. My sincere thanks to all the faculty members and non-teaching staff of the Mechanical Engineering Department who directly or indirectly helped me to carry out this research work successfully.

I would express my sincere thanks to the Surface Engineering Division of CSIR–National Aerospace Laboratories (NAL), Bengaluru, especially Dr. Nirranjan, Dr. P. Kondaiah, and Dr. Venkatramana, who helped me to learn about the development of coatings and working of coating machines. I would like to thank the staff of the Surface Engineering Division of CSIR–National Aerospace Laboratories (NAL), Bengaluru, especially Mr. Praveen, Mr. Siju, and Mr. Srinivas, for their inseparable support and constant help. I thank the Central Instrument Facility Centre (CIFIC) Indian Institute of Technology (BHU), Varanasi, for providing most of the sample characterization instruments. My special thanks to Mr. Girish Sahu for SEM analysis, Mr. Nirmal Mallick for SPM analysis, Mr. Vinay Kumar for TEM analysis, Mr. Durgesh Prasad Gupta for FTIR analysis, Mrs. Pankajini Mohapatra for XPS analysis, Mrs. Payal Sharma for FESEM analysis, Mr. Akhilesh Kumar Paswan and Ms. Smirti Mishra for XRD analysis for their interactions and continuous help during my research work. The office staff of the Central Instrument Facility Indian Institute of Technology (BHU), Varanasi, Mr. Anirban Roy, and Mr. Shiv Charan Saroj for their constant help and support. I would like to thank the staff of the fretting wear group, Division of macro tribology and wear protection, BAM, Berlin

(Germany), for their support during the experimental work. The thanks are also extended to BAM, Berlin (Germany), for extending financial support to carry out the research work.

I am thankful to the office staff of the Mechanical Engineering Department, in particular, Mr. J. K. Sinha, Mr. Akash Mishra, and Mr. Jay Singh, for their constant help and support. Special thanks to the Tribology and Dynamics of Machine Laboratory of the Department staff, Mr. S. P. Singh, and Mr. Rajam Patel for their enthusiastic support.

I am very obliged to my seniors Dr. Sooraj Singh Rawat, Dr. Homender, Dr. Rajeev Nayan Gupta, Dr. Manvendra Kumar Singh, Dr. Shushant Singh, and Dr. Prashant Kumar, for engaging me in fruitful discussions on my research work and encouraging me throughout the work. Special thanks to my colleagues at Tribology Laboratory, Mr. Gulshan Verma and Mr. Rupesh, for sparing their valuable time and efforts in helping me conduct the experiments.

Special thanks to my friends Mr. Pulkit Madaan, Mrs. Dipti, Mr. Harshit, and Mr. Rishav Sinha for supporting me and always making me understand the different aspects of life. I also want to extend my thanks to Mr. Netan, Mr. Manan, Mrs. Mansi, Mr. Arpit, Ms. Saumya, Mr. Bonny, Mr. Varun, Mr. Akash, Mr. Animesh, Ms. Neha, and Ms. Akriti for their support and cooperation that seems difficult to express in words.

I express my heartiest thanks to my parents, Mr. Om Prakash and Mrs. Rita, and my brother Mr. Vishal Vansh for their inseparable support and encouragement at every stage of my academic and personal life. I can never thank them enough for everything they have done for me and everything they continue to do for me. They are truly my inspiration and possibly the best parents a child could have.

Some people came late into my life during the course of my Ph.D. research work but made a great impact during that short period of time. Among those people, the first one is my wife, Mrs. Pooja Singh, who became an integral part of my life, and I would like to thank her for

being my muse, sounding board, and keeping me sane over the past few months. The next ones whom I want to thank are my teammates and juniors with whom I play cricket (Mr. Anurag Sai, Mr. Amitram, Mr. Mohit, Mr. Mayank, Mr. Manish, Mr. Saroj, and others) for showing unconditional love and support during the last phase of my Ph.D. research work.

I would like to thank all other people who have provided a truly conducive environment to successfully carry out this research. My sincere thanks to all those who directly or indirectly put their effort in every bit of completion of the research work. To all these people and to those unmentioned, my heartfelt thanks.

At last, thanks to the Almighty “God” who has given me the author spiritual support and courage to complete this work.

(Amod Kashyap)

*Dedicated to my beloved
grandmothers.*

Abstract

The fabrication of mechanical components depends upon the applications, which call for different materials with different properties. Apart from this, the failure of lubricant properties at elevated temperatures has resulted in the proper selection of materials for various tribological applications. The cost of procurement of these materials and machining them into tools and components is also arduous. Therefore, in tribological contacts at elevated temperatures, it is imperative to select coatings as an alternative for increasing the life of these tools and machinery components.

The design and selection criteria of the coatings are based on different tribological applications. The present study was focused on the tribological responses of multilayer and nanocomposite coatings at elevated temperatures. The multilayer coatings were sputter deposited, while the nanocomposite coatings were polymer-based coatings deposited through spray pyrolysis. The incorporation of the ductile layer between the hard ceramic layers in the multilayer coating not only reduces the internal stress of the coating but also prevents the propagation of cracks from one brittle layer to another. The polymer nanocomposite coatings were prepared by reinforcing them with pristine and alkylated MoS₂ nanosheets to enhance their tribological properties.

The various machine tools and equipment made of SS 304 suffer severe damage from galling while working. Therefore, new coatings are developed to prevent surface damage to avoid galling at room and elevated temperatures. The Mo/DLC coatings were developed to prevent the galling at room and elevated temperatures (around 300°C). All galling tests were conducted on the test rig made in accordance with ASTM G196. The DLC (diamond like carbon) has a mixture of sp² and sp³ hybridized carbon. The deposition of the DLC layer through high power impulse magnetron sputtering (HiPIMS) ensured a high deposition percentage of sp³

hybridized carbon. The soft Mo layer deposited through a pulsed DC power source helped reduce the internal stress and helped in depositing coating with higher thickness. Almost a three-fold increase in the load-bearing capacity was observed in the tribopair, having coated against uncoated samples. A cost-effective way of increasing the galling resistance of SS 304 has also been explored by coating the samples with polyurethane (PU) based nanocomposite coatings. The PU based coatings were reinforced with pristine and alkylated MoS₂ nanosheets to improve their tribological performance. A comparative study has been presented on the reciprocating and galling wear performance of the PU based nanocomposite coatings. The surface of the pristine MoS₂ nanosheets was modified with octadecane thiol (ODT) to form alkylated MoS₂ nanosheets. The PU-MoS₂-ODT coatings showed significant decrease in friction and wear, 77 and 95%, respectively. Furthermore, the galling resistance of PU-MoS₂-ODT coating was better than the plain PU and PU-MoS₂ coatings.

Various characterization techniques were employed to study the properties of the coatings and the worn scar. These include field emission scanning electron microscopy (FESEM), elemental dispersive x-ray analysis (EDAX), Raman spectroscopy, x-ray photoelectron spectroscopy (XPS), nanoindentation, Fourier transform infrared spectroscopy (FTIR), stereo-zoom optical microscopy, and nanoscratch testing.

Contents

CERTIFICATE.....	I
Acknowledgements	IV
Abstract.....	IX
Contents	XI
List of Figures.....	XVIII
List of Tables	XXIV
1. Introduction.....	1
1.1. Tribology.....	1
1.2. Galling.....	3
1.3. Coatings.	4
1.4. Coating methods.	6
1.4.1. Electroplating.....	6
1.4.2. Chemical solution deposition (CSD).	7
1.4.3. Sol-gel.....	7
1.4.4. Dip coating.....	7
1.4.5. Spray coating.	8
1.4.5.1. Air spray coating.....	8
1.4.5.2. Ultrasonic spray coating.	9
1.4.6. Physical vapour deposition (PVD).....	9

1.4.7. Chemical vapour deposition (CVD).	10
1.5. Coating types.....	10
1.5.1. Monolithic Coatings.....	10
1.5.2. Multilayer coatings.	10
1.5.3. Structurally or compositionally graded coatings.	11
1.5.4. Nanocomposite coating.....	11
1.6. Summary.....	14
2. Literature review.	15
2.1. Introduction.	15
2.2. Physical vapour deposition (PVD).....	16
2.3. Diode sputtering.	17
2.4. Magnetron sputtering.	18
2.4.1. Types of magnetron sputtering on the basis of design of cathode.....	19
2.4.2. Types of magnetron sputtering on the basis of power source of cathode.....	22
2.4.2.1 D.C. magnetron sputtering.....	23
2.4.2.2. Radio frequency magnetron sputtering.....	23
2.4.2.3. Pulsed D.C. magnetron sputtering.....	25
2.4.2.4. High power impulse magnetron sputtering.....	26
2.5. Coatings.....	28
2.5.1. Design Criteria.....	29
2.5.2. Influence of structural design parameters on functional properties.....	30

2.6.	Types of coatings.	31
2.6.1.	Hard Coatings.	32
2.6.1.1.	Adaptive mechanism using metal diffusion.	41
2.6.1.2.	Adaptive mechanism using tribo-oxidation.....	43
2.6.1.3.	Adaptive mechanisms using structural transitions.	43
2.6.2.	Solid lubricant coating.	45
2.6.3.	DLC based coatings	47
2.6.4.	Polymer coatings.....	52
2.7.	Methodology of coating selection.	56
2.7.1.	Coating pre-selection.	57
2.7.2.	Basic characterization of coatings.	60
2.8.	Problem formulation.	61
2.8.1.	Motivation.....	61
2.8.2.	Problem definition.	62
2.9.	Objectives of work.	63
3.	Materials and experimentation methodology.....	65
3.1.	Materials.	65
3.1.1.	Sample preparation for various coatings.....	65
3.1.2.	Synthesis of MoS ₂ and MoS ₂ -ODT nanosheets.....	65
3.2.	Coating systems.	67
3.2.1.	Semi-industrial sputtering system.....	68

3.2.2. Laboratory scale balanced sputtering system.	69
3.2.3. Spray pyrolysis equipment.....	70
3.3. Preparation of coatings.	71
3.3.1. PVD coatings.	71
3.3.2. PU-based coatings.....	72
3.4. Characterization of nanosheets.	72
3.4.1. Transmission electron microscopy (TEM).	72
3.4.2. X-ray diffraction (XRD).	73
3.4.3. Fourier transform infrared spectroscopy (FTIR).	73
3.5. Characterization of coatings.	74
3.5.1. Field emission scanning microscopy (FESEM).....	74
3.5.2. Nanoindentation hardness tester.	74
3.5.3. Micro Raman spectrometer.....	74
3.5.4. X-Ray photoelectron spectroscopy (XPS).	75
3.6. Tribological testing.	75
3.6.1. TKLB tribometer (Ball on disc tribometer).	75
3.6.2. Multifunctional tribometer (MFT).	76
3.6.3. Nanoscratch tester and nanotribometer.....	76
3.6.4. Galling tester.	77
3.7. Summary.....	79
4. Study of tribological properties of multilayer Ti/TiN coating containing stress absorbing layers.	81

4.1. Introduction.....	81
4.2. Material and methods.....	83
4.3. Results and Discussion.....	87
4.3.1. SEM analysis of the coated surface.....	87
4.3.2. XRD analysis of the coating.....	89
4.3.3. Tribological performance of the coating.....	91
4.3.3.1. Friction behaviour of the coated surface with lubrication	91
4.3.3.2. Worn surface analysis	92
4.3.3.3. SEM analysis of wear scars	95
4.3.3.4. Raman spectroscopy analysis of wear scar.....	99
4.4. Summary.....	102
5. Study on galling behaviour of HiPIMS deposited Mo/DLC multilayer coatings at room and elevated temperature.....	105
5.1. Introduction.....	106
5.2. Experimental details.....	110
5.3. Results and discussion.....	115
5.3.1 Microstructure of the coating.....	115
5.3.1.1. Cross-section of the coating.....	115
5.3.1.2. Raman and x-ray photoelectron spectroscopy studies of the Mo/DLC multilayer coating.....	116
5.3.2 Mechanical and tribological characterization of Mo/DLC multilayer coating.....	

5.3.2.1. Hardness of the coating.....	122
5.3.2.2. Friction and wear results.....	123
5.3.2.3. Adhesion strength of the optimized coating for galling tests.	124
5.3.2.4. Galling test at RT.....	127
5.3.2.5. Galling test at 300 °C.....	132
5.3.2.6. Comparison of coated and uncoated galled surface.....	137
5.4. Summary.....	141
6. Comparative study on galling and antiwear behaviour of polyurethane based coatings reinforced with pristine and alkylated MoS₂ nanosheets.....	145
6.1. Introduction.....	145
6.2. Materials and methods.....	150
6.2.1. Synthesis and functionalization of MoS ₂ nanosheets.	150
6.2.3. Preparation of PU based nanocomposite coatings.....	151
6.2.4. Characterization of PU based nanocomposite coatings.....	152
6.2.5. Tribological characterization of PU based nanocomposite coatings.....	153
6.3.1. Characterization of MoS ₂ and MoS ₂ -ODT nanosheets.....	155
6.3.2. Characterization of PU based nanocomposite coatings.....	158
6.3.3. Tribological characterization of PU based nanocomposite coatings.....	163
6.3.3.1. Reciprocating friction tests.....	163
6.3.3.2. Galling tests of PU based nanocomposite coatings.....	168
6.4. Summary.....	173
7. Conclusions and scope of future work.....	175

7.1. Conclusions.....	175
7.2. Scope of future work.....	176
References.....	179
Appendix.....	216
List of publications.....	228

List of Figures

Figure 2.1. Schematic representation of PVD technique.....	17
Figure 2.2. Schematic diagram of magnetron sputtering.....	19
Figure 2.3. Schematic diagram representing the formation of plasma in a balanced and unbalanced magnetron sputtering systems.....	21
Figure 2.4. Schematic diagram of top view of unbalanced magnetron sputtering systems having (a) closed-field configuration, and (b) mirror-field configuration.....	22
Figure 2.5. Chemical bonding triangle of hard coatings.....	33
Figure 2.6. Schematics of bilayer structure and deformation regimes of a brittle layer on a thick compliant substrate under axisymmetric indentation (a) thick coating, (b) thin coating, and (c) thin films (reproduced from reference [114]).....	38
Figure 2.7. Schematic representation of chameleon adaptive coatings. Reprinted with permission from reference [126].....	40
Figure 2.8. Schematics of Ag and Au diffusion onto the surface of the coating at high temperatures.....	42
Figure 2.9. Example of friction induced re-orientation and crystallization in W-Mo-Se-S composite coating after a thousand cycles of sliding against SiC fiber tip at room temperature. Reprinted with permission from reference [147].....	44
Figure 2.10. Schematics of wear mechanism in DLC coatings.....	47
Figure 2.11. Common polymer coatings with filler elements. Reprinted from open access reference [201].....	54
Figure 2.12. Wear mechanisms generally occurring in a system.....	57
Figure 2.13. Process of coating pre-selection.....	60

Figure 3.1. Schematic representation of MoS ₂ nanosheets functionalized with ODT. Reprinted with permission from reference [3].	67
Figure 3.2. Semi-industrial sputtering system.	68
Figure 3.3. Laboratory scale balanced sputtering system.	69
Figure 3.4. Spray Pyrolysis Equipment.	70
Figure 3.5. Flowchart of coating fabrication through PVD technique.	72
Figure 3.6. Photograph of the reciprocating sliding tribometer. 1. D.C motor with eccentric adjustment, 2. top arm with integrated load cell, 3. dead weight, 4. rotational arm, 5. vibrating table, 6. steel disk holding unit, 7. heating element and thermocouple holding unit, and 8. Plexiglas chamber (Reprinted with permission from reference [3]).	76
Figure 3.7. Schematics of test samples (Reprinted with permission from reference [7]).	77
Figure 3.8. Schematic representation of the galling test apparatus.	79
Figure 4.1. A typical hysteresis loop of frictional force and displacement.	86
Figure 4.2. Schematic representation of (a) ball on disk arrangement (b) wear scar on flat surface (c) wear scar on the ball.	88
Figure 4.3. The cross-sectional view of ultrathin Ti/TiN coating with SAL. The inset shows the high-resolution image of a Ti/TiN multilayer stack.	88
Figure 4.4. XRD pattern of ultrathin multilayer Ti/TiN coating with SAL.	90
Figure 4.5. TEM image of cross-section of Ti/TiN multilayer coatings.	90
Figure 4.6. Variation of CoF under unlubricated condition (a) at 30 °C, (b) at 100 °C; and lubricated condition (c) at 30 °C, (d) at 100 °C	93
Figure 4.7. Wear volumes under different test conditions.	95
Figure 4.8. (a) SEM image of CWL tested at 100 °C (b) magnified image of the worn surface; EDX elemental mapping of worn surface (c) Ti, (d) N and (e) O.	97

Figure 4.9. SEM images and EDX elemental mapping of (a),(c),(e),(g),(i) CL at 30 °C; (b),(d),(f),(h),(j) CL at 100 °C.	98
Figure 4.10. Raman spectra of coating and worn surfaces.	101
Figure 4.11. Raman spectrum analysis of CL at 100 °C.....	102
Figure 5.1. (a) Setup of galling tester 1) Thermocouple, 2) rotating table, 3) specimen heater, 4) top specimen holder for frictional torque measurement; 1(b) cross-sectional view of aligned samples inside the heater.	115
Figure 5.2. FESEM of cross-section of the Mo/DLC coating.	116
Figure 5.3. (a) Image of the coated and uncoated samples, (b) schematic representation of layers of coating on a galling sample.....	117
Figure 5.4. Raman shift of D and G peaks for coatings prepared at different argon flow rates.	118
Figure 5.5. Deconvoluted spectrum of Mo/DLC multilayer coating deposited at 8 sccm of argon flow rate.	119
Figure 5.6. Variations of (a) I_D/I_G ratio and (b) G peak position with respect to argon flow rate.	119
Figure 5.7. XPS C1s spectra of coating deposited at argon gas flow rates of (a) 12.5 sccm (b) 15 sccm and (c) 18 sccm.	121
Figure 5.8. Load vs displacement curves of Mo/DLC multilayer coatings at different flow rates.	122
Figure 5.9. Coefficient of friction of Mo/DLC multilayer coating deposited at various argon gas flow rates.	124
Figure 5.10. Wear depth profiles of coatings deposited at different argon flow rates.....	125
Figure 5.11. H/E and H^3/E^2 values of Mo/DLC coating deposited at different argon flow rates.	126

Figure 5.12. Acoustic emission data and optical images of the scratch with magnified images of the scratch at bottom.....	128
Figure 5.13. Friction torque curves obtained for the two tribopairs at room temperature at (a) 5 MPa (b) 10 MPa and (c) 15 MPa.....	129
Figure 5.14. Stereozoom microscopic images of the galled samples at RT (a-f) and at 300 °C (g-j).	130
Figure 5.15. (a) FESEM image of the galled sample at 5 MPa load, (b) FESEM image of steel counterpart at 5MPa showing transferred layer, and (c) EDX spectrum of transferred layers.	131
Figure 5.16. Friction torque curves of the tribopairs obtained at 300 °C (a) 2 MPa (b) 5 MPa and (c) 7 MPa.....	134
Figure 5.17. (a) C1s spectrum of the galled sample at 300 °C and (b) Mo3d spectrum of the galled sample at RT and 300 °C.	135
Figure 5.18. (a-h) Stereo-zoom images of galled surface along with their respective processed images (g) plot of galled area across different applied stresses at RT and (h) 300 °C.....	136
Figure 5.19. (a-h) Stereo-zoom images of galled surface along with their respective processed images (g) plot of galled area across different applied stresses at RT and (h) 300 °C.....	138
Figure 5.20. Radial cross-section SEM images of galled surfaces (a) coated and (b) uncoated.	139
Figure 5.21. SEM images of the top surface of the galled surface (a) steel (steel on steel tribopair) (b) uncoated sample (steel on Mo/DLC multilayer coating tribopair) and (c) coated sample (steel on Mo/DLC multilayer coating tribopair).....	139
Figure 5.22. Schematic representation of the mechanism of galling in steel on steel tribopair; (a) asperities come into contact having strong adhesive forces and (b) material transfer and prows being formed.	140

Figure 5.23. Schematic representation of galling mechanism in steel on Mo/DLC multilayer coating tribopair (a) asperities of coated sample and uncoated sample coming into contact, (b) formation of build-up asperity on the uncoated surface, and (c) the strain hardened build up asperity on uncoated surface ploughing the coated surface..... 142

Figure 6.1. Schematic representation of MoS₂ and MoS₂-ODT nanosheets preparation. 150

Figure 6.2. PU coated substrates for (a) reciprocating wear tests, and (b) galling tests. 152

Figure 6.3. Schematic representation of parameters required to calculate specific wear volume of PU based coatings..... 154

Figure 6.4. HRTEM images of (a) and (b) MoS₂, (c) and (d) MoS₂-ODT nanosheets. 155

Figure 6.5. XRD data of MoS₂ and MoS₂-ODT nanosheets..... 157

Figure 6.6. FTIR spectra of MoS₂ and MoS₂-ODT nanosheets..... 157

Figure 6.7. SEM images of cross-section of the (a) PU-MoS₂, (b) PU-MoS₂-ODT coatings; Elemental mapping of Mo in (c) PU-MoS₂, (d) PU-MoS₂-ODT coatings. 158

Figure 6.8. Nanohardness loading and unloading curves of (a) plain PU, (b) PU-MoS₂, and (c) PU-MoS₂-ODT coatings. 159

Figure 6.9. Acoustic emission data of the scratch test of PU based coatings. 162

Figure 6.10. Optical microscopic images of scratches of PU based coatings..... 163

Figure 6.11. Coefficient of friction curves for (a) PU based nanocomposite coatings at 10 N, (b) 20 N, and (c) PU-MoS₂-ODT coating at different loads..... 165

Figure 6.12. (a) Wear profiles of different coatings tested at 10 N in reciprocating testing, and (b) specific wear volume of different coatings at different loads (specific wear volume of the plain PU and PU-MoS₂ coating was not shown for 20 N, as these coatings failed during reciprocating tests). 167

Figure 6.13. Stereozoom microscopic images of wear scar of (a) PU, (b) PU-MoS₂, and (c) PU-MoS₂-ODT coatings tested at 10N load. Optical microscopic images of wear scar of (d) PU, (e) PU-MoS₂, and (f) PU-MoS₂-ODT coatings tested at 10N load. 168

Figure 6.14. Friction torque curves of (a) PU, (b) Pu-MoS₂, and (c) PU-MoS₂-ODT coatings at various loads. 169

Figure 6.15. Stereozoom images of the galled surface of (a) plain PU coating at 10 MPa, (b) PU-MoS₂ coating at 12.5 MPa, and (c) PU-MoS₂-ODT coating at 17.5 MPa. 172

List of Tables

Table 1.1. Properties of various coatings.	13
Table 4.1. Parameters for coating deposition.	84
Table 5.1. Deposition parameters for Mo/DLC coatings for a single layer.	112
Table 6.1. Summary of work reported on galling over the years.	149
Table 6.2. Various properties of PU based nanocomposite coatings.	161
Table 6.3. Maximum Hertzian contact stress for PU-MoS ₂ and PU-MoS ₂ -ODT coatings at various loads.	164
Table 6.4. Number of rotations survived by different coatings before getting galled.	171

Abbreviations/Symbols

Abbreviations	Descriptions
°C	Degree Centigrade
AC	Alternating Current
Ag	Gold
Al ₂ O ₃	Alumina
AlCrN	Aluminium Chromium Nitride
AlN	Aluminium Nitride
Ar	Argon
ASTM	American Society of Testing and Materials
at%	atomic percentage
ATSP	Aromatic Thermosetting Polyester
Au	Silver
C	Carbon
CL	Coated Substrates With Lubrication
CN	Carbon Nitride
CNT	Carbon Nano Tubes
CoF	Coefficient of Friction
Cr	Chromium
Cr ₂ O ₃	Chromium Oxide
CrAlN	Chromium Aluminium Nitride
CrALN	Chromium Aluminium Nitride
CrC	Chromium Carbide

CrCN	Chromium Carbon Nitride
CrN	Chromium Nitride
CVD	Chemical Vapour Deposition
CWL	Coated Substrates Without Lubrication
DC	Direct Current
DCMS	Direct Current Magnetron Sputtering
DLC	Diamond Like Carbon
d_p	Diameter Perpendicular
d_{pa}	Diameter Parallel
E	Elastic Modulus
E'	Reduced Elastic Modulus
EDAX	Elemental Dispersive X-Ray Analysis
EP	Epoxy Resin
eV	Electron Volt
Fe	Iron
FESEM	Field Emission Scanning Electron Microscopy
FTIR	Fourier Transform Infrared Radioscopy
GLC	Graphite Like Carbon
Gpa	Giga Pascal
H	Hardness
HiPIMS	High Power Impulse Magnetron Sputtering
h_{min}	Minimum Film Thickness
ICDD	International Centre for Diffraction Data
JCPDS	Joint Committee on Powder Diffraction
La	Lanthanum

MFT	Multifunctional Tribometer
MoN	Molybdenum Nitride
MoO ₃	Molybdenum Trioxide
MoS ₂	Molybdenum Disulphide
MoS ₂ -ODT	Chemically Modified Molybdenum Disulphide with Octadecanethiol
MPA	Mega Pascal
N	Nitrogen
N-DLC	Nitrogen doped Diamond Like Carbon
Ni	Nickel
O	Oxygen
ODT	Octadecanethiol
PA	Polyamide
PbO	Lead Oxide
PDCMS	Pulsed DC Magnetron Sputtering
PEEK	Polyetheretherone
PF	Phenolic Resin
PHBA	poly-hydroxybenzoic Acid
PI	Polyimide
POM	Polyoxymethylene
PPS	Polyphenylene Sulphide
PTFE	Polytetrafluoroethylene
PU	Polyurethane
PVD	Physical Vapour Deposition
R	Radius of Ball
R'	Reduced Radius of Curvature

RF	Radio Frequency
sccm	Standard Cubic Centimeters per Minute
SEM	Scanning Electron Microscopy
Si	Silicon
Si ₃ N ₄	Silicon Nitride
SiC	Silicon Carbide
TaC	Tantalum Carbide
Ti	Titanium
TiAlN	Titanium Aluminium Nitride
TiB ₂	Titanium Boride
TiBN	Titanium Boron Nitride
TiCN	Titanium Carbon Nitride
TiCrN	Titanium Chromium Nitride
TiN	Titanium Nitride
TiO ₂	Titanium Dioxide
UCL	Uncoated Substrates With Lubrication
UHMWPE	Ultra High Molecular Weight Polyethylene
V ₂ O ₅	Vanadium Pentaoxide
VN	Vanadium Nitride
W	Tungsten
W _{lball}	Linear Wear of Ball
W _{lflat}	Linear Wear of Flat Surface
WN	Tungsten Nitride
W _q	Plainmetric Wear
WS ₂	Tungsten Disulphide

wt%	Weight Percentage
WV	Total Volumetric Wear
W_{vball}	Volumetric Wear of ball
W_{vflat}	Volumetric Wear of Flat Surface
XPS	X-Ray Photoelectron Spectroscopy
XRD	X-Ray Diffraction
ZrN	Zirconium Nitride
η_0	Dynamic Viscosity
σ^*	Composite Roughness
λ	Lambda Ratio